Title: Narrowband Interference Suppression using Undecimated Wavelet Packets in Direct Sequence Spread Spectrum Receivers.

Emilia Pardo * (empargo@ia.cetef.csic.es)
Phone: +34 91 561 8806, Fax: +34 91 441 7651
Instituto de Acústica, CSIC, Serrano 144, 28006 Madrid, Spain

Miguel A. Rodríguez-Hernández (marodrig@upvnet.upv.es)
Phone: +34 96 387 9309, Fax: +34 96 387 7309
E.T.S.I. Telecomunicación, Univ. Politécnica Valencia, Camino de Vera s/n, 46022 Valencia, Spain

Juan J. Pérez-Solano (juan.j.perez@uv.es)
Phone: +34 96 354 3562, Fax: +34 96 354 3550
Institut de Robòtica, Univ. Valencia, Polígono de la Coma s/n, 46980 Paterna, Valencia, Spain

Abstract

A new algorithm for narrowband interference suppression in direct-sequence spread spectrum (DS-SS) communications is presented. The algorithm combines the undecimated wavelet packet transform with frequency shifts to confine the interference energy in a subband that is subsequently eliminated. Computer simulation shows a robust performance that appears to be independent of the interference frequency.

EDICS: SPC–j , SPC-m

Index terms: Interference Suppression, Direct Sequence Spread Spectrum, Undecimated Wavelet Packets, TSA.

1. Introduction

Spread spectrum (SS) communication systems have certain interference rejection capacities that make them suitable for transmitting information in congested or noisy channels. Nevertheless, the performance of these systems is strongly degraded by high power interferences. In this context, interference suppression improves the immunity of the system without increasing the bandwidth. Two classes of interference rejection schemes have been extensively used: time domain adaptive filtering [1] and transform domain suppression [2]. Time-domain adaptive filtering can eliminate completely sine-wave interferences, but needs a convergence time to reach the optimal solution. On the other hand transform domain techniques present quick tracking of changing interferences, but their performance

depends on the ability of the transform to confine the interference in a few bins [1].

This article is focused on narrowband interference suppression by transform domain excision. The received signal is represented in the transform domain and the frequency bands that exceed a certain energy threshold are eliminated. In this way, most of the interference energy is removed with low distortion of the desired broadband signal. The inverse transformation is then applied to reconstruct the interference-suppressed SS signal.

A fundamental aspect in the preceding process is the choice of the transform. The objective is to obtain a set of basis functions that generate a compact representation of the interference. Previous approaches were based on the Fourier transform [1], [3], [4] but their performance is limited due to the windowing effect, which spreads the interference energy. Subsequently, more general multichannel filter bank structures were proposed, of which the Fourier transform is a particular case [5]. These transforms offer greater design freedom. Different types of perfect reconstruction multichannel filter banks have been applied to the interference suppression problem, some examples of which are: modulated filter banks [6], paraunitary filter banks [7] and lapped transforms [2].

The wavelet transform [8] has also been employed to eliminate interferences in DS-SS communications [9]. The multiresolution time-frequency decomposition implemented by this transform performs relatively well with various types of interference, but the spectral partition provided is fixed, in the same way as those obtained with multichannel filter banks, and presents similar limitations, such as interband spectral leakage and fixed time-frequency resolution.

An evolution of the wavelet transform is the wavelet packet transform [8]. It provides greater flexibility than previous transforms, offering a variety of unequal bandwidth spectral decompositions. Wavelet packet transform allows the implementation of adaptive algorithms in the sense that they select the best decomposition tree according to the interference frequency location for each processed frame. In this group, the algorithm proposed in [10] deserves special attention. It is called adaptive time-frequency algorithm because interference suppression can be accomplished in the time or the frequency domain. The switch between time and frequency methods depends on the kind of interference to be eliminated. Pulsed interference is eliminated better in the time domain, because its energy is localized in time and expanded in frequency. On the other hand, narrowband interference suppression is easier in the frequency domain because the energy is localized in frequency and

expanded in time. The dual treatment in time or in frequency provides significant performance improvements. When transformation from time to frequency is required, it is carried out by the tree structuring algorithm (TSA) [10]. The TSA employs adaptive subband tree decompositions or wavelet packets. This method has demonstrated superior performance over conventional fixed transforms for narrowband interference suppression [2], [10], but the results are slightly dependent on the interference frequency.

A new algorithm based on wavelet packets for narrowband interference suppression in spread spectrum communications is described here. Its novelty lies in the application of frequency shifts to the SS signal in order to concentrate the interference in a subband and thus eliminate it completely. The method has been successfully applied to frequency hopping and direct sequence SS systems [11], [12]. In this paper, a detailed description of the scheme for interference suppression in DS-SS systems is presented and experimental results confirming the improvements are provided.

2. Interference Suppression Algorithms based on Wavelet Packets

Two algorithms for interference suppression based on wavelet packets are considered in this paper. The first is the TSA [10], which has demonstrated good performance with a variety of interference types. The second is the new Shifted Undecimated Wavelet Packet Transform Algorithm (SUWPTA) [11], [12]. Both algorithms are described in detail below.

A. Tree Structuring Algorithm (TSA)

TSA interference suppression [10] is based on the wavelet packet transform. For each received signal, the TSA selects the best decomposition tree in order to concentrate most of the interference energy in a single subband. The spectral splitting performed at each level can be either dyadic or triadic to provide greater flexibility to the decomposition. Fig. 1 shows an example of a DS-SS signal contaminated with narrowband interference, and the optimum TSA tree for interference suppression.

However, the results of the TSA can vary in relation to the frequency location of the interference, since in practice the filter responses are not ideal, and overlapping occurs near the transition zones. The new algorithm proposed in this paper attempts to solve this problem by guaranteeing that the interference is centred in one of the subbands. For this purpose, the received signal is shifted in frequency prior to the wavelet packet decomposition.

B. Shifted Undecimated Wavelet Packet Transform Algorithm (SUWPTA)

The SUWPTA combines the undecimated wavelet packet transform (UWPT) with frequency shifts of the signal, in order to concentrate the interference energy in one wavelet subband [11], [12].

The UWPT is an oversampled wavelet expansion [13] that carries out the same filtering steps as the wavelet packet transform, but does not downsample the output signal at each level. Due to the fact that the subbands are not decimated, the filters must be modified at each level j in order to cover different zones of the spectrum. For the dyadic case, the filters at level j should be:

$$H_{0,j}(z) = H_0(z^{2^{j-1}}), \quad H_{1,j}(z) = H_1(z^{2^{j-1}}) \tag{1}$$

where $H_0(z)$ and $H_1(z)$ are the frequency responses of the scaling and wavelet filters, $h_0[n]$ and $h_1[n]$.

The SUWPTA is based on the selection of the optimum frequency shift at each decomposition level of the UWPT, in order to centre the interference in a subband. The selection can be made by testing all the possible frequency shifts in the subband, but this implies a high computational cost. Fortunately, the testing process is only necessary at the highest resolution level, $j=J$, as will be shown.

The algorithm begins at the highest frequency resolution level ($j=J$). In the interval of width B_J, K possible frequency shift values are tested in order to select the optimum one. The parameter K establishes a trade-off between performance and cost. If K increases, the interference is more accurately centred, but the computational cost of the algorithm is also increased.

Once the interference is placed in the centre of a subband at level J, for level J-1 it will be placed in either the centre or the boundary of a band, since the pass-band zones of level j are aligned with the pass-band zones and the transition zones of level j-1, as shown in Fig. 2. Thus for levels $j=J$-1, …, 1, the interference will remain in the centre of a subband simply by applying a frequency shift of value $S(j) = 0$ or $S(j) = B_j/2$, where B_j is the width of the subbands at level j. Fig. 2 shows the optimum shift selection process for J=3. Fig. 2(a) shows the original interference and the optimum shift at level 3 $S(3)$ that centres the interference in a subband. Fig. 2(b) represents the interference in the centre of the subband at level j=2, which implies a frequency shift $S(2) = 0$. Finally, Fig. 2(c) is the scenario at level j=1, where the interference has been shifted $S(1) = B_1/2$.

The SUWPTA process can be summarized in the following steps:

1) *Calculation of the optimum shift at maximum level J.* The analytic signal X_J of the input signal X is obtained by applying the Hilbert transform: $X_J = X + i \cdot Hilbert[X]$. For each frequency shift

$S_k(J)$, being $k = 1,2\ldots K$, the following actions are performed in the interval B_J:

1.a) The complex signal X_J with length N is frequency shifted: $X_{J,S_k(J)} = X_J \cdot e^{i2\pi S_k(J)}$.

1.b) $X_{J,S_k(J)}$ is filtered with $H_0(z)$ and $H_1(z)$ to obtain respectively the low-pass subband $W_{J,0,S_k(J)}$, and the high-pass subband $W_{J,1,S_k(J)}$ for the shift $S_k(J)$.

1.c) The energy difference between both subbands is calculated:

$$\Delta E_{J,S_k(J)} = \left\| \sum_{l=0}^{N-1} \left\| W_{J,1,S_k(J)}(l) \right\|^2 - \sum_{l=0}^{N-1} \left\| W_{J,0,S_k(J)}(l) \right\|^2 \right\| \tag{2}$$

1.d) When the interference is centred in one of the subbands, the energy difference is at maximum. Thus, the optimum frequency shift is:

$$S(J) = \left\{ S_k(J) \middle| \max\left(\Delta E_{J,S_k(J)}\right), k = 1,2,\ldots K \right\} \tag{3}$$

1.e) The subband with lower energy between $W_{J,0,S(J)}$ and $W_{J,1,S(J)}$, is the clean subband, so it is saved together with the shift $S(J)$ for the reconstruction process. The other subband containing the interference is the new input vector for the next resolution level, X_{J-1}.

If all the values of $\Delta E_{J,S_k(J)}$, $k = 1,2,\ldots,K$ are below a certain threshold, the interference is too band-wide to be contained in a single pass-band interval at level J, and the algorithm must start at a lower level: $J'=J-1$.

2) *Calculation of the optimum shift at levels* $j=J-1,\ldots,1$. The optimum shift is known: $S(j)= 0$ if X_j comes form $W_{j+1,0,S(j+1)}$, and $S(j)=B_j/2$ if X_j comes from $W_{j+1,1,S(j+1)}$.

3) *Interference Suppression*. When the last level $j=1$ is reached, the output vector X_0 concentrates the interference and it is removed.

4) *Reconstruction of the interference free SS signal.* Using the saved vectors and frequency shifts, the interference free SS signal is synthesised.

C. Computational costs of TSA and SUWPTA

In both algorithms the computational cost is mainly determined by the transform. The cost of a filtering process is equal to NL operations, where N is the length of the input vector and L is the number of filter coefficients. The TSA is based on the wavelet packet transform. Two decompositions are performed at each level in the analysis part, a dyadic and a triadic one. After each filter, the output

is subsampled. Thus the number of operations involved is $2NL\sum_{j=0}^{J}\left(\frac{1}{2}\right)^{j}+3NL\sum_{j=0}^{J}\left(\frac{1}{3}\right)^{j}$, that asymptotically tends to $4NL+4.5NL$. In the same way, in the synthesis part the number of operations is bounded by a value ranging from $4NL$ with dyadic decompositions to $4.5NL$ with triadic decompositions. Therefore the total cost of TSA in the worst case is bounded by $13NL$.

The SUWPTA is based on the UWPT. At each level, a dyadic decomposition is performed, except for the highest level *J* that includes *K* frequency shifts of the input signal, giving *K* dyadic decompositions. Additionally, the complex input signal doubles the number of operations. The cost of each filtering operation is *NL* at all decomposition levels, since the zero filter coefficients are not taken into account in the implementation. Therefore the number of operations involved in the analysis part is $NL\cdot 2\cdot 2\cdot\left((J-1)+K\right)$. In the synthesis process the frequency shift test is not needed, resulting the number of operations $NL\cdot 2\cdot 2\cdot J$, and thus the total cost of SUWPTA is $8\left(J+\left(K-1\right)/2\right)\cdot NL$.

The previous results show that SUWPTA presents a computational cost higher than TSA. It depends on two parameters: the number of levels *J* and the number of frequency shifts *K*, which establish a trade-off between performance and cost.

3. Experimental results

In order to evaluate the performance of the SUWPTA, a simulator modelling a DS/BPSK system with interference suppression was implemented [14] (see Fig. 3). The input data signal is $d(t)=d_m$, $mT_b \le t<(m+1)T_b$, where $d_m\in\{-1,1\}$ is the data sequence and T_b is the bit time interval. On the other hand, the pseudo-noise code is given by $c(t)=c_n$, $nT_c \le t<(n+1)T_c$, $c_n\in\{-1,1\}$ being *Tc* the chip time interval. After the BPSK modulation the transmitted signal is $s(t)=d(t)c(t)\sqrt{2S}\cos(\omega_0 t)$, where ω_0 is the carrier frequency and *S* the signal power. The channel introduces additive white Gaussian noise, $n_{AWGN}(t)$, and narrowband interference, $I(t)$, resulting the received signal: $r(t)=s(t)+n_{AWGN}(t)+I(t)$. In the receiver a new interference suppression block has been included. This block implements the TSA and the SUWPTA in order to compare their respective performances.

Two types of narrowband interferences have been considered: a continuous wave tone and a Gaussian interference with 10% bandwidth of the SS signal. These two types are similar to those presented in [10] for testing the TSA. For all the experiments the signal-to-interference power ratio is

fixed at –20 dB, and the spreading factor is Tb/Tc=63 chips per bit. The results are displayed as a function of the bit error rate (BER) versus the ratio Eb/N_0, where Eb is the energy per bit and N_0 is the variance of the additive white Gaussian noise introduced by the channel.

Three experiments were carried out in order to evaluate the SUWPTA performance and compare it with that of the TSA, which was a reference. The results are presented by means of the BER curves. Experiments 1 and 2 compare three different situations: no suppression, TSA suppression and SUWPTA suppression. In addition, the ideal case of zero interference is also included. Experiment 3 analyses the SUWPTA performance as a function of the interference central frequency.

The filters used for the SUWPTA and for the dyadic TSA decomposition are Daubechies filters with 16 and 32 coefficients respectively. SUWPTA requires lower order filters to obtain a similar performance, since the interference is always placed in the centre of a subband and this relaxes the transition band requirements. For the triadic TSA, the filter coefficients are those proposed in [5]. In all the experiments the number of transmitted bits was 10^7.

A. Experiment 1: In this case continuous wave tone interference is added to the SS signal. Two tone frequencies corresponding to the limit cases for the TSA are evaluated. The first tone, ω_1=0.61π radians, is located in the centre of a band in the corresponding TSA decomposition. The second tone, ω_2=0.587π radians, is located near the transition zone between two bands. In this experiment, the optimum highest resolution levels are J=6 for ω_1 and J=5 for ω_2 using the TSA, and J=8 for both frequencies utilising the SUWPTA.

The BER curves for the first case, ω_1=0.61π radians, are shown in Fig. 4. It can be observed that the results of SUWPTA, TSA and no interference are very similar. The second case with interference frequency ω_2=0.587π radians is presented in Fig. 5. The values of the SUWPTA, the TSA and the ideal curves are again very close. But in this case a slight difference appears for high values of Eb/N_0: the SUWPTA BER is still very close to the ideal, whereas the TSA BER is slightly higher.

The different TSA performance is due to the different interference frequency locations, since ω_2 is closer to the filter transition zone than ω_1. On the other hand, the SUWPTA curves show similar results whatever the frequency, since the interference is always shifted to the centre of a subband.

B. Experiment 2: This experiment includes a narrowband Gaussian interference affecting 10% of the SS signal bandwidth. Simulations are made for two different interference central frequencies:

ω_1=0.06π radians and ω_2=0.527π radians, which represent the optimum and the worst case, respectively, for the TSA. The first interference, with frequency ω_1=0.06π radians, perfectly fits into one of the subbands in the corresponding TSA decomposition with J=3 levels. However, for the second frequency ω_2=0.527π radians, a two-level TSA tree cannot concentrate all the interference energy in a single subband. This can be appreciated in Fig. 6, where the signal spectrum and the two possible TSA decompositions with J=2 levels have been represented. Since the interference cannot be concentrated in a single subband, the decomposition stops at level J=1. On the other hand, Fig. 7 shows the SUWPTA decomposition process for the same interference, with the result that now the total interference is included in one band because it had previously been shifted. In this case, the optimum value for the highest resolution level is J=4.

The results for the first frequency ω_1=0.06π radians are presented in Fig. 8. In this case the SUWPTA and TSA curves coincide and are slightly higher than the ideal curve, because now the eliminated subband is bigger than in the case of the continuous wave tone interference. The BER curves for the second frequency ω_2=0.527π radians are displayed in Fig. 9. The SUWPTA curve is similar to that presented in Fig. 8. On the other hand, the TSA curve is higher. Thus the SUWPTA performance is independent of the interference frequency, whereas the TSA performance varies with the interference frequency.

C. Experiment 3: This experiment evaluates the SUWPTA performance versus the central frequency of the interference. For this purpose, SUWPTA suppression is applied to interferences with different central frequencies, covering the complete range $\omega \in [0, \pi]$. Figure 10 shows the resulting BER for a fixed value Eb/No = 2, with the two types of interferences considered in experiments 1 and 2: continuous wave tone and narrowband 10% bandwidth Gaussian interference. The curves show an almost constant performance for all frequencies.

4. Conclusion

In this paper we have presented the SUWPTA, a new algorithm for narrowband interference suppression in DS-SS systems based on transform domain excision using UWPT. Its novelty lies in the application of frequency shifts to the SS signal in order to place the interference in the centre of one transform subband. Transition zones between subbands are thus avoided and most of the interference energy is confined to a single subband that can be eliminated with low degradation of the

desired signal.

The performance of the algorithm was evaluated by means of computer experiments. A comparison was established with another algorithm based on adaptive subband transforms: the tree structuring algorithm (TSA) proposed in [10], which has already demonstrated excellent performance, superior to that of conventional fixed transforms. The experiments show that the application of the TSA and SUWPTA presents considerable improvement in comparison to the case with no interference suppression. For continuous wave tone interference, the BER curves of both algorithms are very close to the no interference case. For the narrowband Gaussian interference, the experiments show that SUWPTA provides a BER similar to TSA. However, the SUWPTA results appear to be independent of the interference frequency, whereas the TSA performance is dependent on this factor. The price that has to be paid for the constant performance provided by SUWPTA is the inclusion of a shifting process.

References

[1] L.B. Milstein, "Interference Rejection Techniques in Spread Spectrum Communications", Proceedings of the IEEE, vol.76, no.6, pp.657-671, 1988.

[2] A. Akansu and M. J. Medley, Wavelet subband and block transforms in communications and multimedia, Kluwer Academic Publishers, ch.3, 1999.

[3] R.C. DiPietro, "An FFT based technique for suppressing narrow-band interference in PN spread spectrum communications systems", IEEE International Conference on Acoustics, Speech and Signal Processing, pp.1360-1363, 1989.

[4] J.G. Proakis, "Interference suppression in spread spectrum systems," IEEE 4th Int. Symposium on Spread Spectrum Techniques and Applications Proceedings, vol.1, pp.259-266, 1996.

[5] P.P. Vaidyanathan, "Theory and design of M-channel maximally decimated quadrature mirror filters with arbitrary M, having the perfect-reconstruction property", IEEE Trans. on Acoustics, Speech and Signal Processing, vol.ASSP-35, pp.476-492, April 1987.

[6] W.W. Jones and K.R. Jones, "Narrowband interference suppression using filter bank analysis/synthesis techniques", Proc. MILCOM'92, pp.898-902, Oct. 1992.

[7] A. Ranheim, "Narrowband interference rejection in direct-sequence spread-spectrum system

using time-frequency decomposition", IEEE Proc. Commun., vol.142, pp.393-400, Dec. 1995.

[8] S. Mallat, "A theory for multiresolution signal decomposition: the wavelet representation", IEEE Transaction on Pattern Analysis and Machine Intelligence, vol.11, pp.674-693, July 1989.

[9] M.J. Medley, G.J. Saulnier and P.K. Das, "Applications of the wavelet transform in spread-spectrum communications systems", Proc. Third NJIT Symp. Applicat. Subbands Wavelets, March 1994.

[10] M.V. Tazebay, and A.N. Akansu, "Adaptative Subband Transforms in Time-Frequency Excisers for DS-SS Communications Systems", IEEE Trans. on Signal Processing, vol.43, no.11, pp.2776-2782, 1995.

[11] J.J. Pérez, M.A. Rodríguez and S. Felici, "Interference excision algorithm for Frequency Hopping Spread Spectrum based on Undecimated Wavelet Packet Transform", Electronics Letters, vol.38, no.16, pp.914-915, Aug. 2002.

[12] E. Pardo, J.J. Pérez and M.A. Rodríguez, "Interference excision in DSSS based on undecimated wavelet packet transform", Electronics Letters, vol.39, no.21, pp.1543-1544, Oct. 2003.

[13] M. Shensa, "The discrete wavelet transform: Wedding the à trous and mallat algorithms", IEEE Trans. on Signal Processing. vol. 40, pp. 2464-2482, Oct. 1992.

[14] M.K. Simon, Spread Spectrum Communications Handbook, McGraw-Hill, New York, 1994.

Acknowledgement

We would like to thank the anonymous reviewers and the R+D+i Linguistic Assistance Office at the Universidad Politécnica of Valencia for their help in revising this paper. This work has been partially supported by the Spanish Ministry of Science and Technology (project DPI2002-00441 and grant FPI BES-2004-5296).

Figures

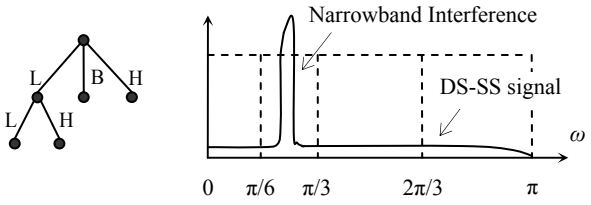

Figure 1. DS-SS signal with narrowband interference and the corresponding TSA decomposition.

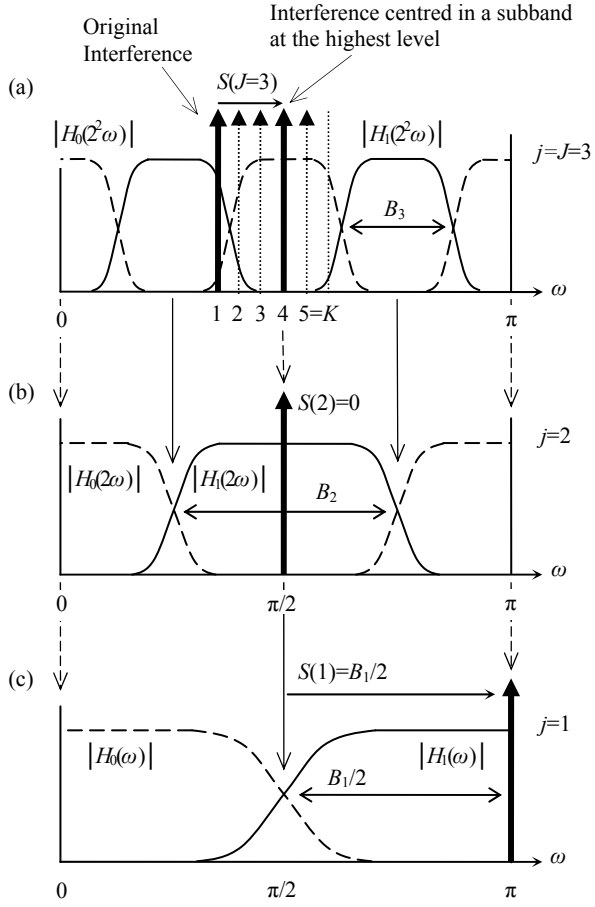

Figure 2. SUWPTA, interference shifting process with J=3. (a) Highest level j=J=3. (b) Level j=2. (c) Level j=1.

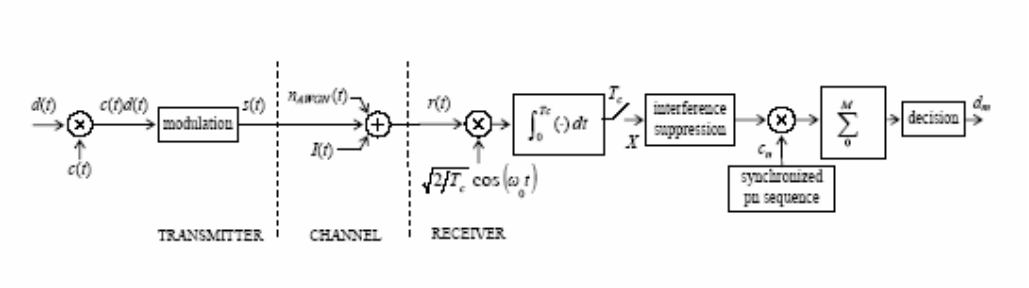

Figure 3. Block diagram of a DS/BPSK system, including interference suppression in the receiver.

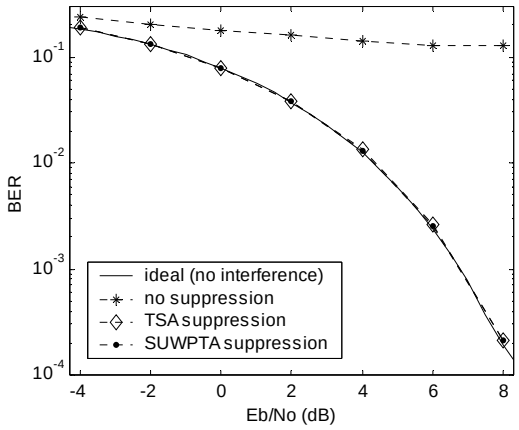

Figure 4. BER curves for the case of continuous wave tone interference with frequency $\omega_1 = 0.61\pi$ radians.

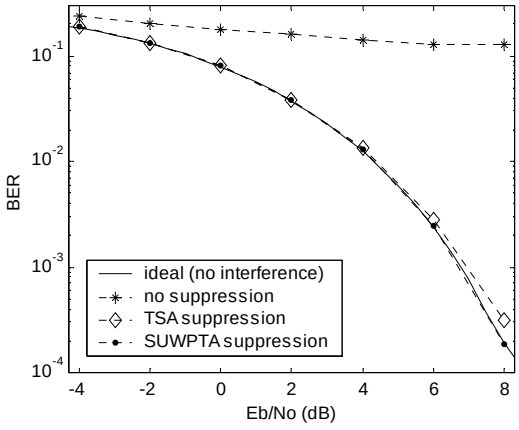

Figure 5. BER curves for the case of continuous wave tone interference with frequency $\omega_2 = 0.587\pi$ radians.

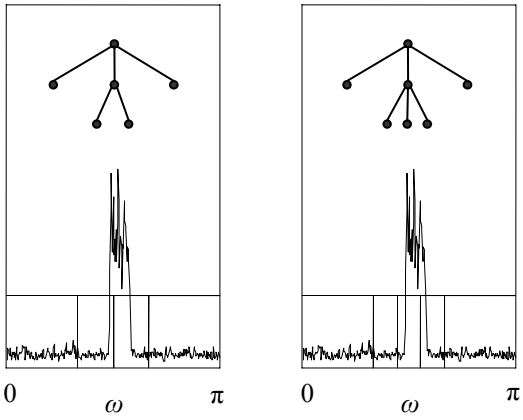

Figure 6. Two possible TSA decompositions for the case of Gaussian interference with 10% bandwidth and central frequency $\omega_2 = 0.527\pi$ radians.

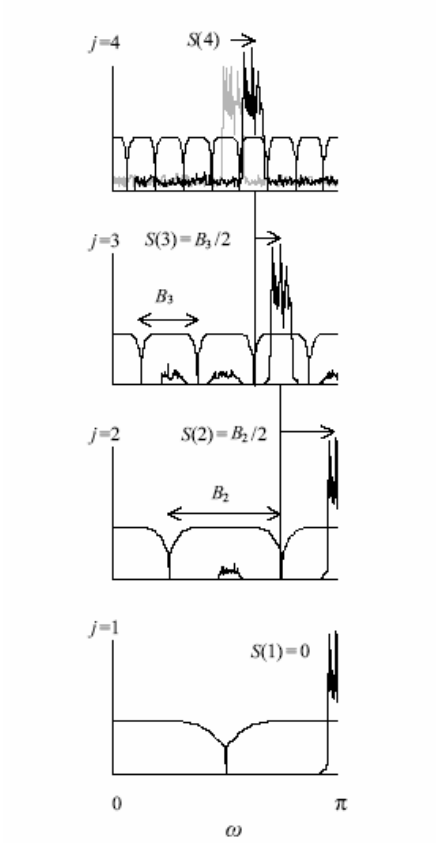

Figure 7. SUWPTA decomposition process for the case of Gaussian interference with 10% bandwidth and central frequency $\omega_2 = 0.527\pi$ radians.

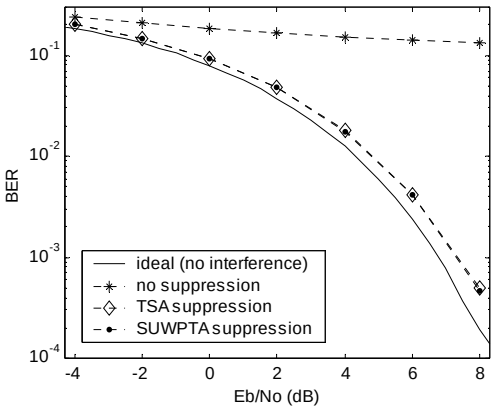

Figure 8. BER curves for the case of Gaussian interference with 10% bandwidth and central frequency $\omega_1 = 0.06\pi$ radians.

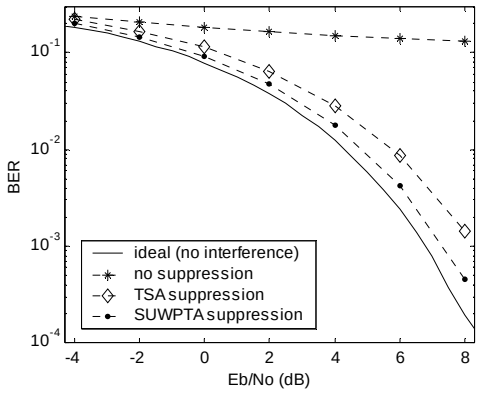

Figure 9. BER curves for the case of Gaussian interference with 10% bandwidth and central frequency $\omega_2 = 0.527\pi$ radians.

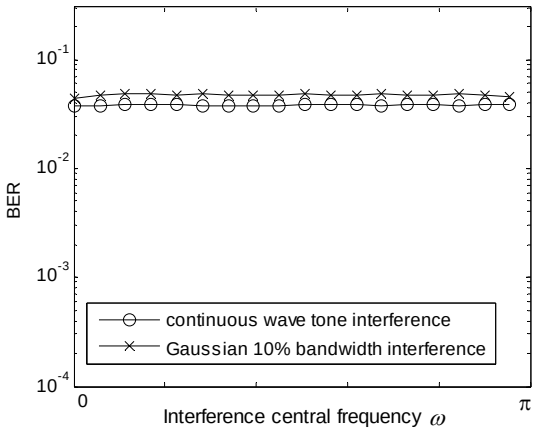

Figure 10. BER versus interference central frequency for the SUWPTA algorithm (Eb/No=2dB in all cases).